Mean secondary electron yield of avalanche electrons in the channels of a microchannel plate detector

H. O. Funsten and D. M. Suszcynsky
Space and Atmospheric Sciences Group, Los Alamos National Laboratory, Los Alamos, New Mexico 87545

R. W. Harper
EG&G Energy Measurements, Los Alamos, New Mexico 87544

(Received 20 May 1996; accepted for publication 10 July 1996)

By modeling the statistical evolution of an avalanche created by 20 keV protons impacting the input surface of a *z*-stack microchannel plate (MCP) detector, the mean secondary electron yield γ_C of avalanche electrons propagating through a MCP channel is measured to equal 1.37 for 760 V per MCP in the *z* stack. This value agrees with other studies that used MCP gain measurements to infer γ_C. The technique described here to measure γ_C is independent of gain saturation effects and simplifying assumptions used in the segmented dynode model, both of which can introduce errors when inferring γ_C through gain measurements. © *1996 American Institute of Physics.* [S0034-6748(96)02110-7]

I. INTRODUCTION

Microchannel plate (MCP) detectors are extensively used to detect and image individual particles such as photons, electrons, and ions. Detection of an incident particle by a MCP detector proceeds as follows.[1–5] An incident particle impacts the input surface of a MCP detector and produces one or more secondary electrons. These electrons are subsequently accelerated down a MCP channel by a channel electric field of ~ 2 MV m^{-1} and impact the channel wall, producing more secondary electrons. This growing electron avalanche propagates down the channel and is detected at the output of the MCP detector.

A crucial parameter that governs the initiation and evolution of the electron avalanche in a MCP detector is the secondary electron yield γ_C resulting from the impact of avalanche electrons on a channel wall. For example, models of MCP operation show that the MCP gain[6–11] and noise[12] are strongly dependent on γ_C.

Previous quantification of the avalanche process utilized the measured MCP detector gain to infer γ_C.[7,8,11,13] To model the multiplication process, the MCP channel is typically represented as a segmented dynode having *m* discrete stages. Assuming the MCP gain is not saturated, the dependence of the MCP channel gain *G* on γ_C can be represented using[7,8]

$$G \approx \gamma_1 \gamma_C^{m-1}, \tag{1}$$

where γ_1 is the mean secondary electron yield of the first collision in the channel. Interestingly, since γ_1 is dependent on the species and energy of the primary particle that impacts the channel wall, measurement of the gain can be utilized as a coarse method to distinguish different particles and energies.[14–16]

Several factors are not included in the segmented dynode model of Eq. (1) but must be considered when inferring γ_C from gain measurements. First, under certain operating conditions, space charge,[17,18] internal electric fields arising from charge depletion from the channel wall,[9,19,20] and strip current limitations at high count rates[21,22] can decrease γ_C near the output end of a channel, resulting in gain saturation. Second, the dynode model assumes that the number of dynode stages *m* is independent of the applied MCP voltage, which is not likely to be valid.[23] Third, γ_1 in Eq. (1) includes events that produce no secondary electrons and, therefore, no avalanche. In pulse counting mode, such events influence the probability of avalanche initiation (and, therefore, the quantum detection efficiency) rather than the gain. Consequently, for pulse counting mode Eq. (1) is valid only if the probability that the primary particle produces no electrons is small. If this probability is significant, then γ_1 must be replaced by the mean number of secondary electrons produced by the primary radiation that includes only events in which the secondary electron yield is one or greater. For example, for UV photons incident on a MCP detector in which $\gamma_1 < 0.1$,[24] avalanches are primarily formed by a single photoelectron so that $G \approx \gamma_C^{m-1}$. In conclusion, when deriving γ_C using gain measurements, γ_1 must be quantified, gain saturation of the MCP must be characterized, and the number of discrete dynode stages *m* must be assumed or derived.

Assuming no gain saturation, the secondary electron yield of avalanche electrons can be described by[7,8,13,25,26]

$$\gamma_C = \left(\frac{V}{m V_C} \right)^k, \tag{2}$$

where *V* equals the voltage applied to the MCP, *k* is a constant that describes the power dependence of γ_C on *V*, and the crossover voltage V_C corresponds to the applied MCP voltage at which $\gamma_C = 1$. Typically, *k* is assumed to equal 0.5, V_C ranges from 20 to 30, and *m* ranges from 10 to 20.[8,11,13] Note that the assumption $k = 0.5$ implies that γ_C is proportional to the mean impact velocity of an avalanche electron.

Instead of deriving γ_C from the measured gain of a MCP detector, we examine the initiation and propagation of an avalanche in a channel to derive a value for γ_C. We employ a variable applied electric field near the input surface of a MCP detector to manipulate the detection of secondary electrons created by an incident particle striking the web of the

 0034-6748/96/67(10)/3478/5/$10.00

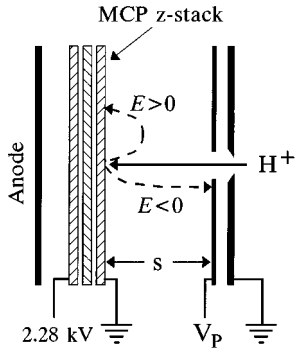

FIG. 1. The experimental apparatus employs an electric field E between the plate biased to V_P and the grounded input surface of the MCP detector to control the detection of web electrons. The dashed lines represent web electron trajectories for the two opposing electric field directions.

MCP input surface.[16,24,27,28] From these measurements, we derive the secondary electron yield γ_C of avalanche electrons.

II. EXPERIMENT

The experimental apparatus used here has been described in detail elsewhere.[16] As shown in Fig. 1, an applied electric field E oriented perpendicular to the input surface of the MCP detector was generated using a conductive plate located a distance s in front of the MCP input surface. We define $E=-V_P/s$, where V_P is the bias of the conductive plate relative to the MCP detector input surface. The MCP detector, which consisted of a z stack of 75 mm diam MCPs, was biased to 2.28 kV (760 V per MCP). Each MCP had a 40:1 channel length-to-diameter ratio, a 5° channel bias angle, front and rear surfaces metallized with Inconel, and a calculated open area ratio, f_{OAR}, equal to 0.63. The detector was stimulated using a 20 keV proton beam that transited a small aperture in the biased plate and struck the MCP detector at normal incidence. A ground plate with an aperture smaller than the aperture in the biased plate was used to define the beam cross-sectional area and to minimize electrostatic effects of the biased aperture plate on beam transport.

III. EXPERIMENTAL RESULTS AND ANALYSIS

The observed count rate $R(E)$ of 20 keV protons striking the MCP detector as a function of the applied electric field E is shown in Fig. 2. Since the applied electric field does not penetrate into MCP channels, the detection efficiency of protons entering channels is independent of E.

However, the trajectories of secondary electrons produced by protons impacting the web, referred to as web electrons or WEs, are strongly dependent on E. For example, for $E\leqslant -1$ V/mm, which we define as E_-, WEs are accelerated away from the MCP input surface, so protons that strike the web are not detected. Thus, only protons entering channels can initiate an avalanche in the MCP detector that results in a valid pulse.

For $E\geqslant 1$ V/mm, which we define as E_+, WEs are suppressed back to the MCP detector, whereupon some enter

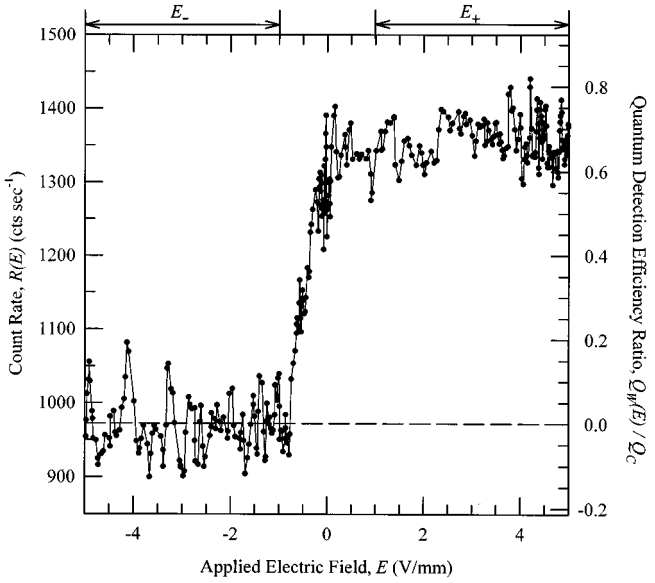

FIG. 2. The measured count rate $R(E)$ of 20 keV protons incident on the MCP detector and the corresponding ratio of the quantum detection efficiencies of protons striking the web to protons striking channels are shown as a function of the applied electric field E. The electric field is divided into regions E_- and E_+ that correspond to $E\leqslant -1$ V/mm and $E\geqslant 1$ mm, respectively.

channels and initiate an avalanche. Thus, in addition to protons entering channels, protons striking the web can be detected. WEs that do not enter a channel reimpact the web at the same energy as their emission energy (typically 2–5 eV) and are assumed to produce no ternary electrons. This assumption is valid due to the small secondary electron yield associated with the low impact energy of WEs striking the web material.

If we assume no loss of real pulses in the detector electronics, then the observed count rate of protons striking the MCP detector is

$$R(E)=\phi A Q_{\mathrm{MCP}}(E), \tag{3}$$

where ϕ is the incident proton flux (protons per unit area and time) striking the detector, A is the cross-sectional area of the proton beam (equal to the beam-defining aperture area), and $Q_{\mathrm{MCP}}(E)$ is the quantum detection efficiency of the MCP detector. We construct Q_{MCP} as the sum of the quantum detection efficiencies of protons striking channels (Q_C) and the web (Q_W):

$$Q_{\mathrm{MCP}}(E)=f_{\mathrm{OAR}}Q_C+(1-f_{\mathrm{OAR}})Q_W(E). \tag{4}$$

Note that Q_C is independent of E since the applied electric field does not penetrate into the channel.[16,24,27]

For E_- WEs are accelerated away from the MCP input surface so that protons striking the web are not detected, i.e., $Q_W(E_-)=0$. Therefore, $R(E_-)=\phi A f_{\mathrm{OAR}}Q_C$ follows directly from Eqs. (3) and (4). Furthermore, by rearranging Eqs. (3) and (4) and substituting $R(E_-)$ for $\phi A f_{\mathrm{OAR}}Q_C$, we obtain

$$\frac{Q_W(E)}{Q_C}=\left(\frac{R(E)}{R(E_-)}-1\right)\frac{f_{\mathrm{OAR}}}{1-f_{\mathrm{OAR}}}. \tag{5}$$

Figure 2 depicts the ratio $Q_W(E)/Q_C$ derived using Eq. (5), where the dashed line corresponds to $R(E_-)=972$ counts s^{-1}, which is the average value of $R(E)$ over the interval -5 V/mm$<E<-1$ V/mm.

For E_+, in which WEs are deflected by the applied electric field back to the MCP detector and can be detected, we obtain an average value of 1355 counts s^{-1}. Equation (5) then yields the result $Q_W(E_+)/Q_C \approx 0.67$.

IV. MODEL OF AVALANCHE EVOLUTION

For electron impact on a channel wall, a Poisson secondary electron yield distribution has been routinely used to characterize MCP avalanche growth.[13,25,29,30] Here, we follow a similar approach and assume that the secondary electron yield of protons impacting the input surface of the MCP detector and avalanche electrons impacting channel walls both follow a Poisson probability distribution $F(n,\gamma)$, where n is the number of secondary electrons created and γ is the mean secondary electron yield. We note that a Poisson representation of secondary electron emission by ion bombardment of metals underestimates the number of interactions having no electron emission,[31–34] although this effect should be small due to the large average secondary electron yield of 20 keV protons on Inconel.

A. Avalanche initiation by particle impact on a channel wall

The probability that incident radiation striking a channel wall initiates an avalanche depends on the mean secondary electron yield γ_1 of the impact event. Avalanche growth depends on the secondary electron yield γ_C of avalanche electrons that impact the channel wall. Statistically, since $\gamma_C=1$ is required to sustain an avalanche, $\gamma_C>1$ is required for the avalanche to grow.

Using Poisson statistics, the probability that an incident particle entering a channel will initiate an avalanche is

$$Q_C=1-\sum_{n=0}^{\infty} F(n,\gamma_1)P_0(n,\gamma_C), \tag{6}$$

where $F(n,\gamma_1)$ describes secondary electron emission of the primary impact. The term $P_0(n,\gamma_C)$, which equals the probability that secondary electrons produced by incident radiation impacting a channel wall will not initiate an avalanche, includes the possibility of avalanche extinction at any point as the avalanche propagates down a channel.

When the avalanche strikes the MCP detector anode, it must have enough charge to register a valid pulse in the subsequent electronics. Therefore, since Eq. (6) does not track the number of electrons in an avalanche, it assumes that an avalanche consisting of a few electrons, as in the case of $\gamma_C \approx 1$, can result in a valid pulse. Typically, pulse-counting electronics are not capable of recognizing such small pulses, especially in the presence of thermal noise. Therefore, we only consider cases for which avalanche growth is significant, i.e., when $\gamma_C \geqslant 1.1$.

We derive values for Q_C as a function of γ_C and γ_1 using a Monte Carlo simulation that tracks the initiation and evolution of an avalanche through an MCP channel that is represented as a series of discrete dynode stages. The simulation, which assumes that secondary electron emission follows Poisson statistics, computes the number of times that an avalanche is extinguished within the first 12 stages for 10^4 primary particles entering the channel. This model overestimates Q_C due to the inability of Eq. (6) to consider the avalanche magnitude as a condition for a valid pulse.

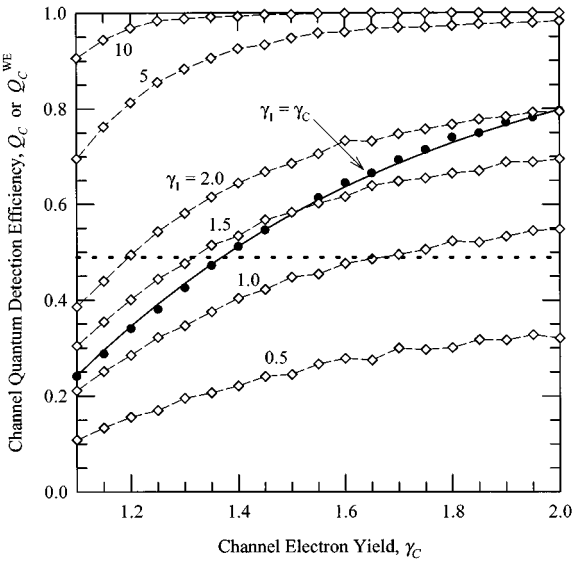

FIG. 3. The probability of avalanche initiation by a primary particle that impacts a channel wall with a secondary electron yield of γ_1 is derived using a Monte Carlo simulation of Eq. (6), where γ_C equals the electron yield of avalanche electrons. The solid line is a fit to the data for $\gamma_1=\gamma_C$. The dotted line is the derived value $Q_C^{\mathrm{WE}}=0.49$ for $Q_W(E_+)=0.67$ and $\gamma_w=3.6$.

Figure 3 shows Q_C as a function of γ_C for various values of γ_1 (open diamonds). As expected, Q_C increases with an increase in either γ_1 or γ_C. The solid line, $Q_C=1-3.82\exp(-1.47\ \gamma_C)$, represents a best fit to the data for which $\gamma_C=\gamma_1$ (solid circles). When $\gamma_C \gg 1$, which corresponds to a high probability of avalanche growth, γ_C approaches a maximum value $1-F(0,\gamma_1)=1-\exp(-\gamma_1)$, which equals the probability that a primary particle impacting a channel wall produces at least one secondary electron.

B. Avalanche initiation by particle impact on the web

When web electrons are repelled back to the input surface of the MCP detector (i.e., for E_+ in Fig. 2), the web quantum detection efficiency is

$$Q_W(E_+)=1-\sum_{n=0}^{\infty} F(n,\gamma_W)(1-P_C Q_C^{\mathrm{WE}})^n, \tag{7}$$

where P_C is the probability that a WE enters a channel, γ_w is the mean secondary electron impacting the web, and Q_C^{WE} equals the probability that a WE produces an avalanche once it enters a channel. The quantity $1-P_C Q_C^{\mathrm{WE}}$ equals the probability that one WE does not initiate an avalanche, and $(1-P_C Q_C^{\mathrm{WE}})^n$ is the probability that none of the n WEs produced by a primary particle impacting the web initiates an avalanche.

Since Eq. (6) describes the channel quantum detection efficiency for any type of primary radiation, we use Eq. (6) to evaluate Q_C^{WE}, which is the channel quantum detection

efficiency for web electrons, by substituting the mean secondary electron yield γ_1^{WE} of WEs impacting a channel wall for γ_1:

$$Q_C^{WE}=1-\sum_{n=0}^{\infty} F(n,\gamma_1^{WE})P_0(n,\gamma_C). \quad (8)$$

In addition to Q_C, Fig. 3 shows Q_C^{WE}.

V. EVALUATION OF γ_C

We first obtain a value for Q_C^{WE} in Eq. (7) and then derive a value for γ_C using Eq. (8) for Q_C^{WE}. In Eq. (7), we know (a) $Q_W(E_+)\approx 0.67\ Q_C$ from the data of Fig. 2 and (b) $\gamma_W=3.6$ for 20 keV protons at normal incidence on Inconel, the web material.[16] The remaining unknown variables required in Eq. (7) for evaluation of Q_C^{WE} are P_C and Q_C, which we now estimate.

The probability that a WE randomly enters a channel is simply equal to the fraction of the input surface consisting of channels, i.e., $P_C=f_{OAR}=0.63$. This is valid for the electric field magnitude used in this study (1 V/mm$<E<$5 V/mm), which is strong enough to repel WEs back to the input surface of the MCP detector but is weak enough so that WEs do not impact the detector close to their point of origin, thereby maximizing ''lensing'' of the WEs into channels.[10] From Eq. (7), we note that a variation in the value of P_C results in an inversely proportional variation in Q_C^{WE}.

Next, we expect that $Q_C\approx 1$ due to the large secondary electron yield resulting from protons striking a channel wall. For 20 keV protons at normal incidence on Inconel, the mean secondary electron yield was measured to be $\gamma_W=3.6$.[16] A considerably larger secondary electron yield γ_1 is expected for 20 keV protons impacting channel walls due to the dielectric channel wall material[35,36] and the glancing angle of incidence, for which γ_1 scales as $\cos^{-\alpha}\theta$, where θ is the angle of incidence relative to the surface normal and α is close to unity for light ions.[35,37–39] For a channel bias angle of 5°, we expect an enhancement in the secondary electron yield of ~11.5 due to the grazing angle of incidence (85°) of protons striking a channel wall. Therefore, we expect $\gamma_1>10$, so we obtain $Q_C\approx 1$ from Fig. 3 for $\gamma_C>1.1$. This is consistent with studies indicating that $Q_C\approx 1$ for keV ions striking channels.[40–42]

For $Q_W(E_+)=0.67\ \ Q_C$, $\gamma_w=3.6$, $P_C=0.63$, and $Q_C=1$, we use Eq. (7) to obtain $Q_C^{WE}=0.49$, which is depicted as the dotted line in Fig. 3. Now, we focus on Eq. (8) to describe Q_C^{WE}, and the unknown variables are γ_1^{WE} and γ_C.

While the trajectories of WEs are quite complex due to the complicated electric field structure near the channel throats, we assume that WEs entering channels are indistinguishable from avalanche electrons, i.e., $\gamma_1^{WE}\approx\gamma_C$, for the following reasons. First, WEs are emitted with a similar energy distribution, peaked at several eV, as channel secondary electrons. These WEs enter a channel at this low energy, equivalent to emission of avalanche electrons at a wall. Second, the channel electric field at the channel throat steers these low energy WEs toward trajectories parallel to the channel axis. This compensates for the possibility that a WE can enter a channel at a location near the central axis.

TABLE I. Comparison of derived values of the avalanche secondary electron yield γ_C.

Source	γ_C	Method	Comments
This study	1.37	Avalanche extinction	z-stack configuration; $V=760$ V per plate
Schagen[a]	$\leqslant$1.65	Gain	Upper bound
Eberhardt[b]	1.4	Gain	$V=738$ V, $m=16.2$
Eberhardt[c]	1.32	Gain	Average for all configurations
Eberhardt[c]	1.34	Gain	Average for all z-stack configurations
Giudicotti *et al.*[d]	1.37	Gain	$V=700$ V, $m=11.6$

[a]Reference 13.
[b]Reference 7.
[c]Reference 8.
[d]Reference 11.

Using Eq. (8) with $\gamma_1^{WE}\approx\gamma_C$ and $Q_C^{WE}\approx 0.49$ along with the Monte Carlo simulation results represented in Fig. 3, we obtain $\gamma_C=1.37$. For comparison, Table I shows the secondary electron yield derived from studies using measurements of the MCP gain. Table I also lists the parameters used in these studies to derive γ_C, including the MCP potential V and the assumed number of discrete stages m. Schagen[13] derived a maximum value of γ_C based on an optimal channel length to diameter ratio, and the values of γ_C from Eberhardt[8] represent an average for all MCP operating parameters.

The value of γ_C derived here using the avalanche extinction technique agrees with previous derivations of γ_C using MCP gain measurements. In particular, it equals the value of Giudicotti *et al.*[11] and is only 2.2% more than the average value of $\gamma_C=1.34$ obtained using the z-stack results of Eberhardt.[8]

The derivation of γ_C by following the probability of avalanche extinction as the avalanche propagates down a channel yields an overestimate of γ_C since the model does not consider the avalanche magnitude at the exit of the MCP detector that is required to register a valid pulse in the electronics. However, this overestimation is most significant for $\gamma_C\approx 1$ and should be small for the derived value of $\gamma_C\approx 1.37$.

The avalanche extinction technique described here for deriving γ_C has several advantages over derivation of γ_C by gain measurements. The gain technique requires accurate knowledge of γ_1, an assumption of the number of the discrete dynode stages, and quantification of gain saturation, which can be especially significant in the z-stack configuration if a large number of electrons enter a single channel in the second or third MCP.[43] While γ_1 is not accurately known in this study, we have used incident 20 keV protons so that γ_1 is large enough to justify $Q_C\approx 1$. Therefore, derivation of γ_C in the avalanche extinction technique is independent of the specific value of γ_1. Furthermore, the avalanche extinction method is independent of the gain and the number of dynodes, so that quantification of gain saturation and assumptions of the number of dynode stages are not required.

ACKNOWLEDGMENTS

The authors gratefully thank J. Baldonado and D. Everett for their laboratory support. This work was performed under the auspices of the United States Department of Energy.

[1] J. L. Wiza, Nucl. Instrum. Methods **178**, 587 (1979).
[2] J. G. Timothy, Publ. Astron. Soc. Pac. **95**, 810 (1983).
[3] O. H. W. Siegmund and R. F. Manila, in *Multichannel Image Detectors*, edited by Y. Talmi, ACS Symposium Series 236 (American Chemical Society, New York, 1983), Vol. II, pp. 253-273.
[4] M. A. Gruntman, Instrum. Exp. Tech. (USSR) **27**, 1 (1984).
[5] G. W. Fraser, *X-ray Detectors in Astronomy* (Cambridge University, Press, Cambridge, 1989), Chap. 3.
[6] J. Adams and B. W. Manley, IEEE Trans. Nucl. Sci. **NS-13**, 88 (1966).
[7] E. H. Eberhardt, Appl. Opt. **18**, 1418 (1979).
[8] E. H. Eberhardt, IEEE Trans. Nucl. Sci. **NS-28**, 712 (1981).
[9] G. W. Fraser, J. F. Perason, G. C. Smith, M. Lewis, and M. A. Barstow, IEEE Trans. Nucl. Sci. **NS-30**, 455 (1983).
[10] G. W. Fraser, Nucl. Instrum. Methods **206**, 445 (1983).
[11] L. Giudicotti, M. Bassan, R. Pasqualotto, and A. Sardella, Rev. Sci. Instrum. **65**, 247 (1994).
[12] B. N. Laprade, S. T. Reinhart, and M. Wheeler, Proc. SPIE **1243**, 162 (1990).
[13] P. Schagen, Adv. Image Pickup Display **1**, 1 (1974).
[14] M. E. Gruntman, Instrum. Exp. Technol. (USSR) **28**, 157 (1985).
[15] D. G. Mitchell, A. F. Cheng, S. M. Krimigis, E. P. Keath, S. E. Jaskulek, B. H. Mauk, R. W. McEntire, E. C. Roelof, D. J. Williams, K. C. Hsieh, and V. A. Drake, Opt. Eng. **32**, 3096 (1993).
[16] H. O. Funsten, D. J. Suszcynsky, R. W. Harper, J. E. Nordholt, and B. L. Barraclough, Rev. Sci. Instrum. **67**, 145 (1996).
[17] D. A. Bryant and A. D. Johnstone, Rev. Sci. Instrum. **36**, 1662 (1965).
[18] K. C. Schmidt and C. F. Hendee, IEEE Trans. Nucl. Sci. **NS-13**, 100 (1966).
[19] D. S. Evans, Rev. Sci. Instrum. **36**, 375 (1965).
[20] C. Loty, Acta Electron. **14**, 107 (1971).
[21] G. W. Fraser, M. T. Pain, J. E. Lees, and J. F. Pearson, Nucl. Instrum. Methods Phys. Res. A **306**, 247 (1991).
[22] G. W. Fraser, M. T. Pain, and J. E. Lees, Nucl. Instrum. Methods A **327**, 328 (1993).
[23] W. B. Feller, IEEE Trans. Electron Devices **ED-32**, 2479 (1985).
[24] R. C. Taylor, M. C. Hettrick, and R. F. Malina, Rev. Sci. Instrum. **54**, 171 (1983).
[25] A. J. Guest, Acta Electron. **14**, 79 (1971).
[26] I. P. Csorba, Appl. Opt. **19**, 3863 (1980).
[27] J. A. Panitz and J. A. Foesch, Rev. Sci. Instrum. **47**, 44 (1976).
[28] G. W. Fraser, M. A. Barstow, J. F. Pearson, M. J. Whitely, and M. Lewis, Nucl. Instrum. Methods **224**, 272 (1984).
[29] G. W. Fraser, Nucl. Instrum. Methods **195**, 523 (1982).
[30] M. Ito, H. Kume, and K. Oba, IEEE Trans. Nucl. Sci. **NS-31**, 408 (1984).
[31] C. F. G. Delaney and P. W. Walton, IEEE Trans. Nucl. Sci. **NS-13**, 742 (1966).
[32] G. Lakits and H. Winter, Nucl. Instrum. Methods B **48**, 597 (1990).
[33] K. Ohya and I. Mori, J. Phys. Soc. Jpn. **61**, 2569 (1992).
[34] K. Ohya, F. Aymayr, and H. Winter, Phys. Rev. B **46**, 3101 (1992).
[35] J. Schou, Scan. Microsc. **2**, 607 (1988).
[36] D. Hasselkamp, in *Particle Induced Electron Emission II*, Springer Tracts in Modern Physics, Vol. 123 (Springer, Berlin, 1992), pp. 66–68.
[37] J. Ferrón, E. V. Alonso, R. A. Baragiola, and A. Olivia-Florio, Phys. Rev. B **24**, 4412 (1981).
[38] B. Svensson, G. Holmén, and A. Burén, Phys. Rev. B **24**, 3749 (1981).
[39] B. Svensson and G. Holmén, J. Appl. Phys. **52**, 6928 (1981).
[40] R. S. Gao, P. S. Gibner, J. H. Newman, K. A. Smith, and R. F. Stebbings, Rev. Sci. Instrum. **55**, 1756 (1984).
[41] T. Sakurai and T. Hashizume, Rev. Sci. Instrum. **57**, 236 (1986).
[42] K. Tobita, H. Takeuchi, H. Kimura, Y. Kusama, and M. Nemoto, Jpn. J. Appl. Phys. **26**, 509 (1987).
[43] G. W. Fraser, Nucl. Instrum. Methods A **291**, 595 (1990).